

UC Davis

UC Davis Previously Published Works

Title

Plant and animal PR1 family members inhibit programmed cell death and suppress bacterial pathogens in plant tissues

Permalink

<https://escholarship.org/uc/item/7vp0j0pt>

Journal

Molecular Plant Pathology, 19(9)

ISSN

1464-6722

Authors

Lincoln, James E
Sanchez, Juan P
Zumstein, Kristina
et al.

Publication Date

2018-09-01

DOI

10.1111/mpp.12685

Peer reviewed

Plant and animal PR1 family members inhibit programmed cell death and suppress bacterial pathogens in plant tissues

JAMES E. LINCOLN , JUAN P. SANCHEZ†, KRISTINA ZUMSTEIN‡ AND DAVID G. GILCHRIST *

Department of Plant Pathology, University of California, Davis, CA 95616, USA

SUMMARY

A role for programmed cell death (PCD) has been established as the basis for plant–microbe interactions. A functional plant-based cDNA library screen identified possible anti-PCD genes, including one member of the PR1 family, designated P14a, from tomato. Members of the PR1 family have been subject to extensive research in view of their possible role in resistance against pathogens. The PR1 family is represented in every plant species studied to date and homologues have been found in animals, fungi and insects. However, the biological function of the PR1 protein from plants has remained elusive in spite of extensive research regarding a role in the response of plants to disease. Constitutive expression of P14a in transgenic tomato roots protected the roots against PCD triggered by Fumonisin B1, as did the human orthologue GLIPR1, indicating a kingdom crossing function for PR1. Tobacco plants transformed with a P14a-GFP fusion construct and inoculated with *Pseudomonas syringae* pv. *tabaci* revealed that the mRNA was abundant throughout the leaves, but the fusion protein was restricted to the lesion margins, where cell death and bacterial spread were arrested. *Vitis vinifera* grapes expressing the PR1 homologue P14a as a transgene were protected against the cell death symptoms of Pierce's disease. A pull-down assay identified putative PR1-interacting proteins, including members of the Rac1 immune complex, known to function in innate immunity in rice and animal systems. The findings herein are consistent with a role of PR1 in the suppression of cell death-dependent disease symptoms and a possible mode of action.

Keywords: GLIPR, pathogenesis-related, PCD, Pierce's disease, plant disease, PR1, *Xylella*.

INTRODUCTION

Programmed cell death (PCD) is a vital process for the regulation of growth and development in plants and animals, and is

responsible for cell death in response to pathogen attack, as well as various forms of abiotic stress (Ashida *et al.*, 2011; Dickman and de Figueiredo, 2013; van Doorn and Woltering, 2005; Lam, 2004). The understanding of plant PCD has progressed from initial reports of conserved morphological similarities to apoptosis in animals (Gilchrist, 1998), to the demonstration of cross-kingdom functionality of animal PCD activators and inhibitors in plants (Elmore, 2007; Lincoln *et al.*, 2002; Richael *et al.*, 2001). However, the genetic and molecular mechanisms regulating PCD in plants, although functionally conserved, are still poorly understood, especially compared with the understanding of apoptosis in animals (Dickman *et al.*, 2017; Fuchs and Steller, 2011; Saraste and Pulkki, 2000). Published information from our laboratory established that specific transgenes from homologous or heterologous hosts can block PCD during plant disease development (Harvey *et al.*, 2008; Lincoln *et al.*, 2002) and arrest both symptom development and microbial growth *in planta* in a range of plant–microbe interactions (Gilchrist *et al.*, 2001; Lincoln *et al.*, 2002). Further, we have demonstrated previously that transgenic tomatoes expressing the animal baculovirus-derived anti-apoptotic gene p35 are protected against PCD caused by sphinganine analogue mycotoxins (Fumonisin B1, FB1) and block the localized cell death symptoms caused by infection of *Pseudomonas syringae* pv. *tomato* in susceptible tomatoes (Lincoln *et al.*, 2002). Collectively, these results suggest the existence of cross-kingdom conservation of common pathways and regulatory genes in the activation or suppression of PCD in animal and plant cells.

Plants are known to possess inducible and preformed mechanisms to resist disease (Jones and Dangl, 2006; Lindsay *et al.*, 1993). Amongst the inducible responses associated with resistance to potential pathogens is the synthesis of a wide array of proteins, some of which are referred to as pathogenesis-related (PR) proteins (van Loon, 2006; van Loon and van Strien, 1999). PR proteins were first discovered in tobacco leaves that developed necrotic local lesions after inoculation with *Tobacco mosaic virus* (TMV) (van Loon and van Kammen, 1970), the lesions of which are now characterized as a form of PCD (Reape *et al.*, 2008). However, there is no confirmatory evidence of the direct functional role of PR proteins in inhibiting pathogens *in planta* or indirectly affecting the susceptibility of a plant to pathogen effectors.

The first described PR protein, designated as PR1 in tobacco (later as P14a in tomato), is now recognized to occur as a family of proteins (Fig. 1) and is represented in every plant species

*Correspondence: Email: dggilchrist@ucdavis.edu

†Present address: Monsanto Company, Woodland, CA 95695, USA.

‡Present address: Department of Plant Science, University of California, Davis, CA 95616, USA.



Fig. 1 Alignment of pathogenesis-related 1 (PR1)-like amino acid sequences from plant and animal sources. Sl, tomato (*Solanum lycopersicum*) P14a; Vv, grape (*Vitis vinifera*) PR1; Hs, human (*Homo sapiens*) GLIPR1; Ac, dog hookworm (*Ancylostoma caninum*) PR1 homologue. Alignment was performed by Vector NTI (Life Technologies, Carlsbad, CA, USA) and uses the following conventions: Cn is the consensus of three or more amino acids at the same position and is yellow if all five sequences are conserved and blue if two or more are conserved; green, homologous substitution.

studied to date, with homologues found in animals (Gibbs *et al.*, 2008), fungi (Schuren *et al.*, 1993; Schwab *et al.*, 2005; Teixeira *et al.*, 2012) and insects (Arca *et al.*, 2005). In spite of a long history and cross-kingdom presence of PR1 family members, the biological function of PR1 proteins remains unknown. PR1 mRNA expression has been used extensively as a marker for disease resistance in plants (Glazebrook, 2005) without evidence of the presence of the protein or a direct effect on either the disease or pathogen dynamics. A few reports have indicated that tobacco and tomato PR1 basic proteins have antifungal activity (Niderman *et al.*, 1995) and, more recently, an enhancement of plant resistance against phytopathogenic bacteria and an oomycete has been reported for both *Arabidopsis thaliana* and *Nicotiana tabacum* plants overexpressing the basic PR1 homologue from *Capsicum annuum* (Davletova *et al.*, 2005; Sarowar *et al.*, 2005). In both cases, it was suggested, without direct evidence distinguishing cause vs. effect, that the enhanced resistance is a result of the modulation of reactive oxygen species (ROS) production and/or signalling events. Although the functional role(s) of PR1 in either development or the stress response remains unclear, the importance of this gene, and presumably the protein product to plants, is underscored by the fact that no knockout mutants lacking PR1 have been annotated in any plant database. We use the designation PR1 to represent this class of proteins, and P14a when referring to the specific tomato protein.

Here, we report that an anti-PCD functional assay identifies several members of the PR1 family from various plant species, and orthologues of human and dog hookworm inhibit FB1-induced PCD. Furthermore, we demonstrate that the expression of PR1 as a P14a-GFP (green fluorescent protein) fusion is confined to areas immediately adjacent to the edge of lesions caused by the bacterial pathogen, the location of which is consistent with a function in the reduction of lesion expansion and bacterial titre. In addition, transgenic grapes expressing P14a, the tomato PR1 homologue, show protection against PCD-dependent Pierce's disease. Finally, several putative PR1 interactors have been identified by *in planta* co-immunoprecipitation (Co-IP) with anti-P14a antibodies. Interestingly, many of these interactors have been shown to be part of an innate immune complex in rice, which may suggest that PR1 regulates the activity and/or integrity of the Rac1 complex which results in PCD inhibition.

RESULTS

Transgenic expression of PR1 suppresses FB1-induced PCD in tomato hairy roots

Previously, we have reported that a functional anti-PCD screen of tomato and grape cDNAs leads to the isolation of a number of candidate anti-PCD effector genes (Harvey *et al.*, 2008). The

Table 1 Transgenic tomato root Fumonisin B1 (FB1) susceptibility assays.

Construct	Expressed insert	Accession # of insert	Results on 300 nm FB1
CB5-P14LD	Tomato PR1 (P14a)	P04284	Alive at 6 weeks
CB5-SLPR1-2	Tomato PR1	M69247	Alive at 6 weeks
CB5-VVPR1-1	Grape PR1a	AJ536326	Alive at 6 weeks
CB5-VVPR1-2	Grape PR1	AM481964	Alive at 6 weeks
CB5-AtPR1	Arabidopsis PR1	AT2G14610	Alive at 6 weeks
CB5-GLIPR	Human PR1-like (GLIPR1)	AF400440	Alive at 6 weeks
CB5-MSP	Plant nematode PR1-like	AF013289	Alive at 6 weeks
CB5-AASP	Dog hookworm PR1-like	AF089728	Alive at 6 weeks
CB5-MisS_P14	Frame shift P14a mutant	KT895376	Dead by 2 weeks
Empty vector	No expressed transcript	Not applicable	Dead by 2 weeks
CB5-P35	Baculovirus P35	M16821	Alive at 6 weeks
CB5-P14:GFP	Fusion of P14a and GFP	KT895375	Alive at 6 weeks

FB1-sensitive tomato (*asc/asc*) was transformed with the listed constructs by *Rhizobium rhizogenes* to induce roots. The roots were assayed on Murashige and Skoog (MS) agar containing 300 nm FB1 as described in Experimental procedures.

in planta functional screen was based on the overexpression of genes from a cDNA library by *Rhizobium rhizogenes*-mediated transformation, producing what is commonly known as the hairy root phenotype. The infection results in the induction of multiple transformed roots from vegetative tissue sections of tomato cotyledons following co-cultivation with the transforming bacteria. Each emerging root is an independent transformation event, which contains a single new DNA insert that can be re-isolated by polymerase chain reaction (PCR) for characterization. Consequently, transformed roots that survived treatment with a PCD inducer (300 nm FB1) were recovered by PCR and subjected to a BLAST search. Subsequent repetition of the cDNA screen with different source RNAs resulted in the recovery of a specific PR1 homologue (P14a in tomato, #P04284; grape PR1a, #AJ536326), and is shown in Table 1.

As a constitutively expressed sequence, the P14a gene was very effective in suppressing FB1-induced cell death where protein translation occurred (Fig. 2). For example, at the conclusion of the standard 10-day assay period, the P14a transformed roots survived FB1 treatments (Fig. 2B), whereas the empty vector (EV) control transformed roots were killed within 5 days (Fig. 2A). The control tissue has previously been shown in this assay to exhibit various hallmarks of PCD, such as chromatin condensation and ROS production by the dying cells (Harvey *et al.*, 2008). Immunoblots employing anti-PR1 antibodies were negative for the P14a protein in the EV transformed roots (Fig. 2E). In contrast, the surviving P14a transformed roots expressed a positive PR1 band (15 kDa) (Fig. 2E), indicating that the presence of P14a protein is necessary and sufficient for protection against FB1-induced cell death. A second control consisting of a frame shift mutation of

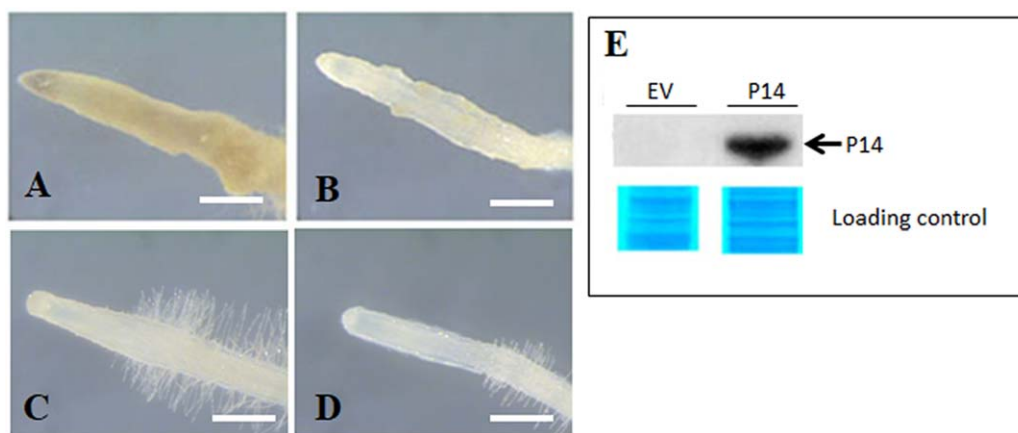


Fig. 2 P14a protects transgenic tomato roots from Fumonisin B1 (FB1)-induced programmed cell death. Transgenic roots were transferred to medium with 300 nm FB1 toxin for 10 days before microscopy. The size bar is 2 mm. (A) Empty vector (EV) control showing dead roots (brown tissue) caused by FB1 treatment. (B) P14a transformant showing protection against FB1-induced cell death. (C) Human GLIPR showing protection against FB1-induced cell death. (D) Dog hookworm PR1 showing protection against FB1-induced cell death. (E) Immunoblots performed on total protein extracts from both EV and P14a hairy roots reveal the presence of P14 solely in the P14 transformants. A portion of the Coomassie-stained gel is shown as loading control.

the P14a coding sequence abolished the protection against FB1 treatment (see Table 1). This further confirms that the P14a protein, and not the mRNA encoding it, is required and responsible for FB1 protection. Subsequently, this protocol was used to investigate whether other plant and animal orthologues of P14a from tomato, grape and *Arabidopsis* would protect against FB1-induced cell death (Table 1). The net result was that each of the P14a orthologue genes listed in Table 1, including the human (GLIPR1) and dog hookworm PR1 orthologues, showed equivalent protection in this functional assay (Fig. 2C,D, respectively), confirming that the anti-PCD activity of the PR1 protein, related to P14a in tomato, is conserved across kingdoms.

Translation of a PR1-GFP fusion protein correlates with cell death induced by *Pseudomonas syringae* pv. *tabaci*

The presence of the PR1 protein from tobacco has been reported to occur in areas immediately adjacent to lesions caused by TMV (Antoniw and White, 1986; Dixon *et al.*, 1991). Reports further suggest (Asai *et al.*, 2000; Stone *et al.*, 2000) that a signal emanating from a dead or dying cell is responsible for the induction of the translation of the PR1 protein in these particular regions. To determine the location of the translated PR1 protein triggered by lesion-limited bacterial disease in relation to these previous reports, *N. tabacum* (tobacco) transgenic plants over-expressing a P14a-GFP fusion protein were infiltrated with *P. syringae* pv. *tabaci*, a well-characterized pathogen of tobacco that is responsible for wild-fire disease (Ribeiro

et al., 1979). Symptomatically, the disease is characterized by the formation of chlorotic halos surrounding necrotic spots on the leaves of infected plants as a result of the induction of PCD by the bacterially secreted tabtoxin (Iakimova *et al.*, 2004). Others have demonstrated that the cell death associated with the secretion of tabtoxin is blocked by pretreatment with tetrapeptide caspase inhibitors (acetyl-asp-glu-val-asp-aldehyde (DEVD-CHO) and others) and the level of ROS is reduced in the protected tissues (Dixon *et al.*, 1991; Elmore, 2007; Richael *et al.*, 2001). Given the results in Fig. 1 indicating that PR1 has anti-PCD activity in the *R. rhizogenes*-based hairy root assay, we reasoned that the expression of PR1 protein might be localized in cells in which lesion expansion is curtailed and bacterial multiplication is confined. Lesion development and the presence of the fusion protein were monitored by confocal microscopy in the inoculated regions (Fig. 3). The confocal images reveal that the fusion protein is restricted to areas adjacent to the lesion borders (Figs 3B,C and S1, see Supporting Information), but not at a short distance from the edge of the lesion (Fig. 3B, top panel).

Furthermore, the area in which the P14a-GFP version of PR1 is present bounds the area in which bacteria are confined and lesion expansion ceases. Northern blots performed on tissue collected from the imaged areas shown in Fig. 3B confirmed that the full-length mRNA of the P14a-GFP fusion protein was present throughout the entire leaf lamina (Fig. 3E), compared with the area in which the P14a protein was restricted. Taken together, these results are consistent with the presence and movement of an activating signal emanating from bacterial effectors, or dying cells, that

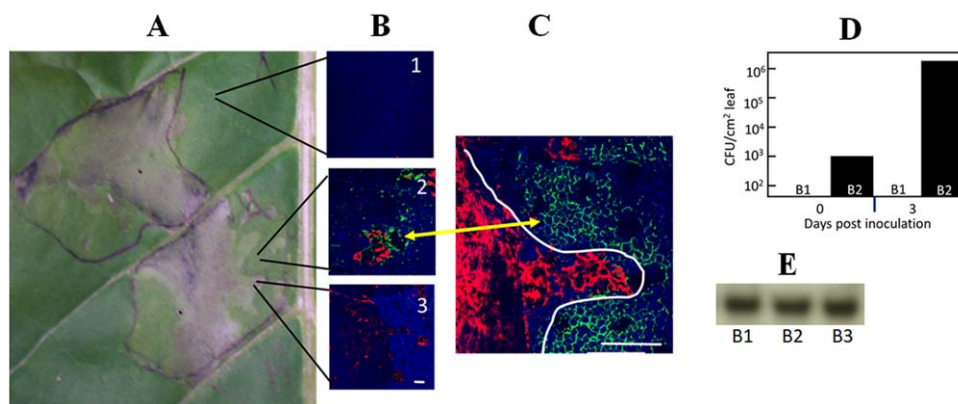


Fig. 3 Expression of P14-GFP fusion protein is localized to the margin of lesions caused by the bacterial pathogen *Pseudomonas syringae* pv. *tabaci*. (A) Close-up of the leaf panels inoculated with *P. syringae* pv. *tabaci* at 3 days post-inoculation (dpi). Panels were inoculated with 1×10^5 colony-forming units (CFU)/mL. The black line outlining the lesion area defines the water-soaked area of infiltration of the bacterial suspension. (B) Confocal microscopy images of outside of the bacterial infiltration zone (1), at the margin of the infiltration zone (2) and the region inside the infiltrated zone (3). Chlorophyll autofluorescence is depicted as blue, dead or dying cells are shown as red and the expression of P14a-GFP fusion protein is shown as green. Size bar is 250 μ m. (C) Close-up of panel B2 showing the presence of the P14-GFP protein in the apoplast of living mesophyll cells (green) adjacent to dead cells (red) that define the margin of the lesions (white line) caused by the presence of the bacterial pathogen. Size bar is 250 μ m. (D) Bacterial growth was analysed at the time of inoculation (0 dpi) and at 3 dpi from leaf tissue sampled from regions B1 and B2. Data are means of three replicate samples per leaf from two experiments. (E) Northern analysis confirms the uniform presence of the transgenic P14-GFP RNA transcript in samples from the three regions denoted in (B).

activates the localized translation of the P14a-GFP fusion protein. Alternatively, the P14a-GFP fusion protein and/or the mRNA encoding it could move from a dying cell towards the lesion boundary. Previously, bacterial titres were measured both inside and outside the lesion boundary at 3 days post-inoculation (dpi) in a leaf panel infiltrated with the anti-apoptotic tetrapeptide DEVD-CHO which was co-inoculated with *P. syringae* pv. *tabaci* (Richael *et al.*, 2001). The analysis indicated that the bacterial population was up to six-fold higher inside the lesion than at the lesion margin, and bacteria did not move beyond the lesion margin. Hence, the suppression of cell death by the apoptotic inhibitor was sufficient to block lesion expansion and confined the bacterial growth inside the lesion without leading to the death of the bacteria. These earlier results are consistent with the localization of the PR1 protein and bacteria, as shown in Figs 3D and S1. This experiment was repeated more than 10 times with the consistent presence of the translated P14a-GFP protein limited to the lesion margin.

Thompson seedless grape plants expressing P14a exhibit suppressed symptoms of Pierce's disease and lower *Xylella fastidiosa* titres

Transgenic grape plants (*Vitis vinifera*) expressing the tomato P14a gene (orthologue of the grape PR1a gene) were generated (Agüero *et al.*, 2015) and tested for their ability to suppress PCD-dependent symptoms associated with Pierce's disease caused by the bacterium *Xylella fastidiosa* (*Xf*). During the course of the experiment, the plants were monitored visually for symptoms and by quantitative PCR (qPCR) for *Xf* bacterial movement and titre. The mean bacterial load of unprotected control plants reached a level of 10^8 bacterial cells per 100 mg stem tissue, and showed symptoms of Pierce's disease after 3 months, with complete leaf death by 6 months (Fig. 4). Both the transgenic and naturally asymptomatic endophytic *Xf* host (*Vitis californica*) plants remained asymptomatic with bacterial titres ranging from 10^2 to 10^4 cells per 100 mg of stem tissue in the main canes of the

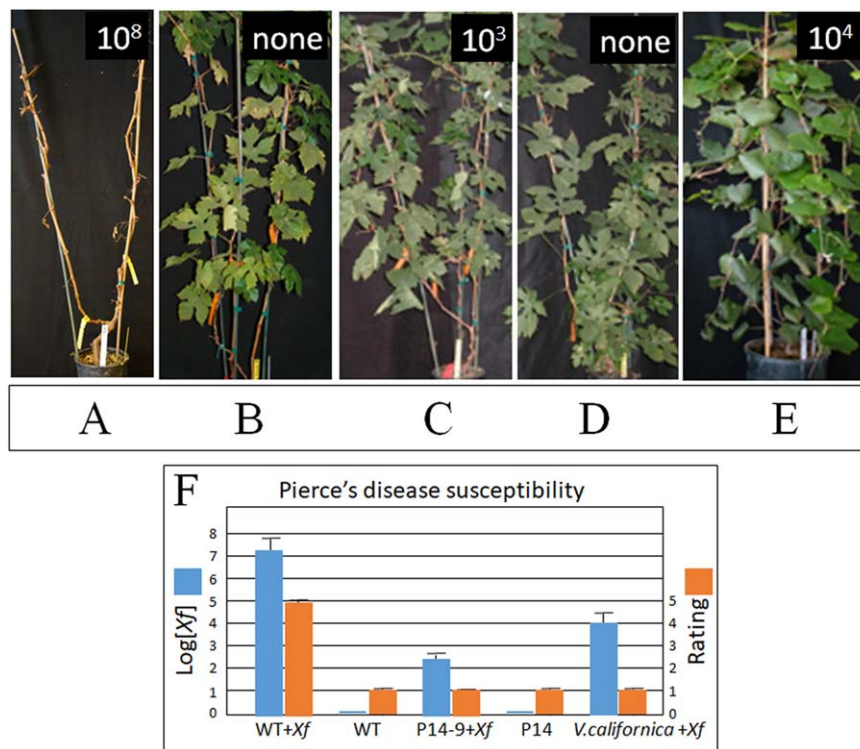


Fig. 4 Pierce's disease evaluation of glasshouse-grown transgenic *Vitis vinifera* cv. Thompson Seedless or *Vitis californica* plants. Two stems of five replicate glasshouse-grown grape plants of the indicated genotypes were mechanically inoculated with 2×10^6 *Xylella fastidiosa* (*Xf*) cells in 20 μ L or mock inoculated with water. Bacterial counts were determined by quantitative polymerase chain reaction (qPCR) for *Xf* DNA, given as cells/100 mg stem tissue (numbers in white), and rated for Pierce's disease symptoms at 3 months post-inoculation. Plants A–E, representing the five glasshouse-grown genotypes listed, were photographed 6 months after inoculation at which point the control plants were dead and the transgenic plants plus *V. californica* remained asymptomatic. (A) Non-transgenic (wild-type, WT) *Xf*-inoculated plant contained 10^8 *Xf* cells/100 mg stem. (B) Non-transgenic, mock-inoculated plant contained no detectable *Xf* DNA. (C) P14-9 *Xf*-inoculated plant contained 10^3 *Xf* cells/100 mg stem. (D) P14-9 mock-inoculated plant contained no *Xf* DNA. (E) *Vitis californica* plant contained 10^4 *Xf* cells/100 mg stem at the time of sampling and remained asymptomatic throughout the course of the experiment. (F) Bacterial titre (*Xf* DNA) of the five inoculated, replicated, glasshouse-grown grape plants of each listed genotype determined by qPCR at 3 months post-inoculation. The rating scale of 1–5 (1, healthy; 5, near death) was recorded at 3 months. The rating results remained the same at 6 months when photographs (A–E) were recorded.

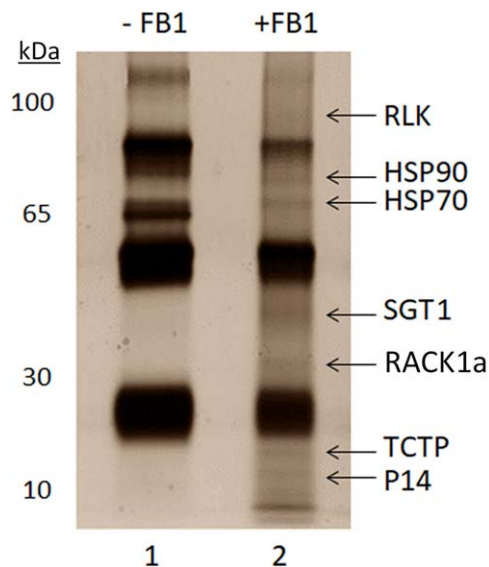


Fig. 5 Members of the Rac1 immune complex are putative P14a interactors. Silver-stained sodium dodecylsulfate-polyacrylamide gel electrophoresis (SDS-PAGE) of total protein extracts from –FB1 (lane 1) and +FB1 (lane 2) treatments subjected to P14a co-immunoprecipitation (Co-IP). Seven differential bands were excised (see arrows) from the gel, trypsin digested and the protein content of each single band was analysed using peptides identified using liquid chromatography-tandem mass spectrometry (LC-MS/MS). Proteins indicated on the gel correlate with the size shown and are amongst the primary proteins identified in the corresponding gel analysis (see Table 2). Equivalent locations from the –FB1 treatments were excised for analysis using LC-MS/MS. Proteins that have been identified previously as being part of the Rac1 immune complex (HSP90, HSP70, SGT1 and RACK1a) are indicated by arrows (see Fig. 6), together with other proteins involved in cell death-related processes (receptor-like kinase (RLK), translationally controlled tumor protein (TCTP)). Table S1 (Supporting Information) shows the complete dataset of all proteins identified by mass when compared with the Solgenomics *Solanum lycopersicum* database (March 2014 version).

inoculated plants at 3 months (Fig. 4) and 6 months (data not shown).

P14a (PR1) interacts with multiple proteins in the Rac1 immune complex

Co-IP experiments, followed by liquid chromatography-tandem mass spectrometry (LC-MS/MS) analysis, were used to identify tomato proteins that interact with the P14a protein in cells undergoing PCD. Total leaf protein was extracted from both FB1-treated and water control tomato leaves and applied to a column to which a P14a-specific antibody had been immobilized. Column-bound proteins were eluted, separated by sodium dodecylsulfate-polyacrylamide gel electrophoresis (SDS-PAGE) and visualized by silver staining (Fig. 5). Seven differentially expressed bands in the FB1-treated sample were then subjected to LC-MS/MS analyses for identification by comparison with the

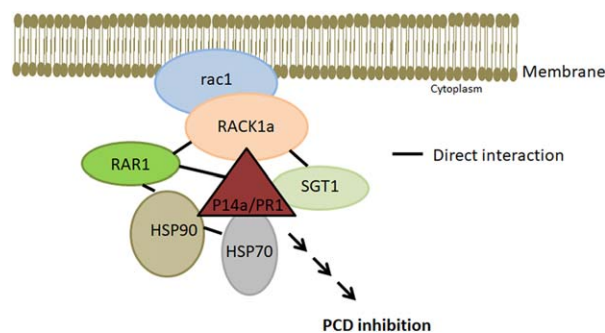


Fig. 6 Model for the P14a protein interaction. P14a interacts with various members of the RACK1a-containing immune complex: HSP70, HSP90, RACK1a and homologue of receptor for Mla12 resistance (RAR1). Rac1 is a small signaling G protein (GTPase). The site of this interaction is unknown [figure based on the model depicted in Nakashima *et al.* (2008)]. A direct protein–protein interaction between HSP70 and GLIPR1, which has been implicated in the control of apoptosis, has been shown (Li *et al.*, 2013). By directly interacting with members of this complex, P14a could regulate their activity and/or integrity within this complex, resulting in the inhibition of programmed cell death.

Solgenomics database (Fig. 5). As expected, no P14a protein was detected by LC-MS/MS in the water-treated control samples. Proteins associated with the Rac1 complex/innate immunity, cell death and/or PR proteins are listed in Tables 2 and S1 (see Supporting Information). Equivalent regions from the no FB1 treatment did not show any of the proteins listed in Table 2, including P14a (Table S1). Of particular interest from the proteomic analysis were several proteins with high search scores that have been shown to be involved in innate immunity in rice by forming part of the Rac1 complex (Nakashima *et al.*, 2008), including suppressor of G2 allele of SKP1 (SGT1), heat shock protein 70 (HSP70) and heat shock protein 90 (HSP90), all of which have been reported to interact with each other and have been proposed to play an important role in innate immunity in rice (Nakashima *et al.*, 2008).

DISCUSSION

PR1 relationship to disease and abiotic stimuli

PR1 has been used widely for more than two decades as a molecular marker associated with plant resistance to a wide range of pathogens, including purported links to systemic acquired resistance (SAR), but no known function has been resolved for the protein. Our interest in the PR1 family proteins arose when it was consistently recovered in a cDNA screen for plant genes that could prevent the death of cells triggered to die by FB1, a fungal-derived activator of apoptosis in both animal and plant cells (Clouse and Gilchrist, 1987; Gilchrist, 1997; Wang *et al.*, 1996). Specifically, P14a, a PR1 homologue from tomato, was identified as a novel PCD inhibitor. Interestingly, PR1 orthologues in both plant and animal species also provided protection against FB1-

Table 2 P14 antibody pull-down analysis of programmed cell death proteins related to innate immunity resolved from tomato plants treated with Fumonisin B1 (FB1).

Category	Protein	Accession no.	Molecular weight (kDa)*	No. of peptide hits [†]	% coverage [‡]
Innate immunity	Heat shock protein 70	Solyc09g010630.2.1	71	57	42
	Guanine nucleotide-binding protein β subunit (ATARCA1; RACK1a)	Solyc06g069010.2.1	36	2	6
	Heat shock protein 90	Solyc07g065840.2.1	80	38	9
	Disease resistance response protein	Solyc10g055200.1.1	21	2	8
	Hop-interacting protein	Solyc12g099930.1	44	9	15
	SGT1	Solyc03g007670.2.1	41	4	12
Cell death	BCL-2 binding anthogene-1 apoptosis regulator BCL2 protein	Solyc10g085290.1.1	38	2	5
	TCTP: Translationally controlled tumour protein	Solyc01g099770.2.1	19	12	57
	Subtilisin-like protease	Solyc10g084320.1.1	83	34	25
	Cathepsin B	Solyc02g069090.2.1	39	5	14
PR proteins	Pathogenesis-related leaf protein 6	Solyc006174340.1.1	18	55	57
	Pathogenesis-related protein PR1 allergen V5 Tpx-1 related	Solyc09g006010.2.1	13	13	41

Liquid chromatography-tandem mass spectrometry (LC-MS/MS) analysis of resolved individual protein bands following sodium dodecylsulfate-polyacrylamide gel electrophoresis (SDS-PAGE) was used to identify proteins differentially present in the plants treated with FB1, compared with untreated tissues. A total of seven FB1 treatment-specific bands were visualized by silver staining (see the designated bands in Fig. 5) and sent for analysis. Equivalent regions from the no FB1 treatment were also analysed.

*Molecular weight of the matching protein.

[†]Number of sequenced peptides that match an identified tomato protein.

[‡]How much of the matching protein is covered by the array of sequenced peptides.

induced cell death (Table 1) in tomato cells. Sequence comparison of PR1 orthologues within genome databases using the CLUSTALW algorithm confirmed a high conservation of several domains in orthologues of the gene analysed from humans, dog hookworm, *Meloidogyne incognita*, grape, tomato and alfalfa (Fig. 1). These included the 'Ancylostoma-secreted proteins' or ASPs that belong to a family of related nematode-specific, cysteine-rich secreted proteins (CRISPs) belonging to the PR1 superfamily. Although, the function of ASPs is unknown, the dog hookworm larval ASPs are released specifically during the transition to parasitism, when cells being fed upon must remain viable. Similarly, in each animal case, the location at which the expression of the respective PR1 orthologue has been reported to be induced is the site at which apoptosis is blocked or suppressed. In reviewing reports of plant responses to disease, the presence of the PR1 signal consistently appears in situations in which the induction of PCD during the compatible infection process is a dependent step and where blocking of cell death is related to resistance (Conrath, 2011; Görlach *et al.*, 1996; Iwai *et al.*, 2007). Similarly, the regulation of PCD plays a key role in mediating plant responses to various cell death-associated events, such as senescence, disease and environmental stresses (van Loon, 1997; van Loon *et al.*, 2006).

PR1 protein localization in relation to cell death

Furthermore, localized expression of the PR1 protein in cells triggered to undergo PCD leads to the suppression of pathogen growth and to the confinement of bacteria to a zone surrounding

the lesion (Richael and Gilchrist, 1999). Similarly, the altered expression of anti-apoptotic transgenes in the current experiments did not kill the pathogen, but restrained the titre in asymptomatic transgenic grape plants from a lethal level of 10^8 to a level of 10^4 – 10^2 cells/g stem tissue in the most resistant lines. Coincidentally, the 10^4 titre is equivalent to the titre measured in the endophytic grape host *Vitis californica* at 3 months after inoculation (Fig. 4), which remained asymptomatic after 6 months, although the bacteria were still present (data not shown).

The activity of this specific PR1 protein in relation to plant disease was further evaluated by infecting tobacco plants overexpressing P14a-GFP RNA with *P. syringae* pv. *tabaci* (Fig. 3). The results of this experiment suggest that translation of the PR1 protein in transgenic tobacco (*N. tabacum*) limits lesion expansion and bacterial growth, presumably by reducing the food base afforded by the cells dying by PCD. The location of the P14a-GFP fusion protein is consistent with a role in the limitation of lesion expansion and growth of *P. syringae* pv. *tabaci* at the lesion margin as a result of the ability of the PR1 protein to block tabtoxin-induced cell death. In the same context, it has been shown that co-infiltration of tetrapeptide caspase inhibitors (i.e. PCD inhibitors) with *P. syringae* pv. *tabaci* in tobacco results in reduced plant cell death and a virtual cessation in bacterial growth (Elmore, 2007; Richael *et al.*, 2001). Together, these results indicate that necrotrophic plant-pathogenic bacteria benefit from the induction of PCD in infected tissues, thereby obtaining nutrients from dying cells. Furthermore, in the current experiments, the location of the translated PR1 protein is consistent with the report by Antoniv

and White (1986), who found PR1 protein only in the areas adjacent to the local lesions where the highest levels of TMV viral particles were confined.

Dixon *et al.* (1991) reported a differential localization of PR1 proteins in the extracellular spaces of tobacco leaves on TMV infection and found that PR1 protein also accumulated within the vacuoles of crystal idioblast cells. Subsequently, infiltration of FB1 into transgenic plants harbouring the PR1 promoter fused to the β -glucuronidase (GUS) reporter gene (Asai *et al.*, 2000) found that PR1-GUS was restricted to the cells surrounding the lesions. This expression is consistent with local, short-distance signals emanating from cells undergoing cell death that trigger the translation of the PR1 protein. Similar results were shown by Chandran *et al.* (2010), using essentially the same strategy, indicating that PR1 transcriptional events in *Arabidopsis* leaves subject to infection by powdery mildew are site specific and only occur in cells immediately adjacent to the site at which the fungus is located; the consequence is to block cell death and permit live cell-dependent nutrient acquisition by haustoria of the obligate parasite. Other reports have shown the expression of PR1 in different systems without consideration of the relationship to stress-related situations (Gu and Innes, 2012; Pečenková *et al.*, 2017; Watanabe *et al.*, 2013). Hypersensitive response lesions have been shown to express NPR1-GFP fusion protein localized to the region surrounding the lesion, where the bacterial pathogen is found (Fu *et al.*, 2012). Furthermore, NPR1 is a positive transcriptional regulator of PR1 (Dong, 2004; Kinkema *et al.*, 2000); therefore, the localization of the NPR1 protein relative to the lesion margin is consistent with our results, which revealed the PR1 protein at the lesion margin, and with translational events dependent on signalling related to PCD. The same pattern of protein translation is shown in Figs 3 and S1, with the highest amounts of translated fusion protein observed in a zone of cells at the border of the non-expanding lesion and inside the cells in which the living bacteria are confined (Fig. 3). Figure S1 confirms that the bacteria exist inside the lesion and not outside the lesion on the healthy portions of the leaf.

PR1 interactive proteins

In order to shed light on the anti-PCD mechanism of PR1, a Co-IP assay was designed to identify proteins that interact with P14a in cells undergoing PCD. PR1 antibodies were used to bind proteins from tomato protein extracts obtained from leaves that had been induced to die by treatment with FB1. This experiment was repeated three times, with several putative PR1 interactive proteins exhibiting a high frequency of recovery (see Fig. 5 and Table 2). These proteins were those previously reported to be part of the innate immunity-associated Rac1 complex (Li *et al.*, 2013). The Rac1 complex has been studied in a number of plant-pathogen model systems for interacting proteins by several methods, including yeast two-hybrid assay, co-IP with antibodies

and fluorescence labelling and microscopy, which support a model involved in innate immunity in rice (Nakashima *et al.*, 2008; Shirasu, 2009). Our analysis showed a direct interaction of this specific PR1 with proteins in this complex, including receptor for activated C kinase 1a (RACK1a), SGT1, HSP70 and HSP90. Numerous members of this complex are implicated in many biological processes, including protein translation, hormonal responses, development, pathogen resistance, environmental stress responses and miRNA production. Significantly, RACK1 is a conserved eukaryotic scaffold protein reported to regulate signal transduction pathways, including cell division, response to environmental stress and response to pathogens, by interacting with diverse proteins (Dongping *et al.*, 2013; Islas-Flores *et al.*, 2015). Plant SGT has been shown to be required for resistance (*R*) gene-mediated disease resistance, non-host resistance and PCD (Azevedo *et al.*, 2006; Peart *et al.*, 2002; Wang *et al.*, 2010). In addition, plant Hsp70 and Hsp90 have been shown to be present in an immunity complex with SGT (Kadota and Shirasu, 2012; Shirasu, 2009), as well as in human cells, where GLIPR1 interacts with HSP70 in prostate cancer cell lines (Li *et al.*, 2013).

The pull-down results presented here include proteins integral to the Rac1 complex (Fig. 6) and are consistent with the immunity complex model in plants, as suggested by Nakashima *et al.* (2008). In this scheme, PR1 directly binds to one or several of the proteins in the Rac1 complex, and, by doing so, alters or blocks downstream signalling events in lipid rafts leading to PCD. The proposed interaction between PR1 and members of the Rac1 complex could occur within the plasma membrane, as homologues of PR1, together with the immune complex, have been detected in lipid rafts, also referred to as detergent-resistant membranes (DRMs) (Fujiwara *et al.*, 2009). Therefore, it is hypothesized here that the accumulation of the PR1 protein, either by protein stabilization or translational regulation, would promote the interaction between PR1 and RACK1a, SGT1, HSP90 or HSP70, which could prevent downstream signalling events that modulate PCD.

PR1 suppression of PCD with pathogen confinement

The results shown here demonstrate that PR1 has the capacity to inhibit PCD induced by FB1 in tomato and to limit Pierce's disease in transgenic grape. In addition, transgenic plants overexpressing a P14a-GFP fusion define lesions caused by *P. syringae* pv *tabaci* by blocking PCD at the lesion boundary. This suppression of PCD supports the results with anti-apoptotic tetrapeptides in tobacco, tomato and bean. In these cases, the suppression of cell death was associated with a dramatic reduction in bacterial titre, but not complete elimination of the bacteria. In fact, the bacteria not only remained alive as a benign endophyte, but were still pathogenic when transferred to a new susceptible plant (Richael *et al.*, 2001).

Although the precise anti-PCD mechanism of PR1 remains unclear at the molecular level beyond association with the Rac1 complex, the data provided here suggest the following: (i) transgenic expression of PR1 can suppress PCD in tomato and grape cells triggered chemically or by pathogens; (ii) the gliocarcinoma orthologue of PR1 (GLIPR) can suppress PCD in plant tissues; (iii) the association of PR1 with the Rac1 complex is consistent with a kingdom-crossing role of this complex in altering cell death-dependent pathways in both plants and animals. In summary, the data herein are consistent with a functional role of PR1 in suppressing PCD in lesion-limited bacterial diseases, whilst permitting the bacteria to remain in an asymptomatic localized endophytic association.

EXPERIMENTAL PROCEDURES

Transgenic tomato (hairy root) production

Tomato seeds were surface sterilized, plated in Magenta boxes and placed in an incubator at 23 °C. *Rhizobium rhizogenes* was transformed with the corresponding construct (Table 1), plated on selective plates, grown for 2 days at 29 °C in liquid 1:1 mannitol glutamate broth + Luria-Bertani medium (MG/L) + kanamycin (Kan) medium and then grown overnight to an optical density at 600 nm (OD₆₀₀) of 0.2–0.4. A cauliflower mosaic virus 35S (CaMV 35S) promoter was used to drive expression. An EV plasmid was used as a control. Tomato cotyledons were cut and immediately immersed in bacterial solution for 20 min, blotted onto sterile Whatman (Maidstone, England) paper and transferred onto Murashige and Skoog (MS) plates (Murashige and Skoog, 1962). Cotyledons were transferred to MS + 200 µg/mL cefotaxime (Cef) + 50 µg/mL Kan plates after 3 days of co-cultivation at 23°C (Harvey *et al.*, 2008).

FB1 screen in hairy roots

Two similar assays were used to identify FB1-resistant transgenic roots. The first method used root tip browning to discriminate between dead roots and survivors, which possess white tips and continued growth (Fig. 2). Fourteen days after transformation, plates containing the P14a-transformed cotyledons with emerging hairy roots (length, 1–4 cm) were flooded with 3 mL of 250 nM FB1. After 10 days of exposure to FB1, surviving roots were transferred to a fresh plate of MS + Cef + Kan + FB1 and incubated for an additional 10 days. EV transformed roots were included as controls and were dead by the end of the second 10-day exposure to FB1 (Harvey *et al.*, 2008). The second method (Table 2) consisted of transferring transformed roots to plates containing 300 nM FB1 for 10 days, which were then moved to a second plate containing 300 nM FB1 for 10 days to complete the screen.

FB1 treatment of tomato seedlings

Four-week-old tomato plants of the FB1-sensitive *asc/asc* genotype (Clouse and Gilchrist, 1987) were grown in growth rooms in a 16-h light and 8-h dark cycle. The seedlings were cut and placed in a beaker containing 500 nM FB1 in water. After 48 h, noticeable lesions began to form on

the leaves. Total protein was extracted as described in Serino and Deng (2007).

PR1 DNA constructs

Plant PR1 genes have no known introns, and so PCR was performed on genomic DNA using primers derived from the published GenBank sequences (see Table 1 for accession numbers and Table 3 for primer sequences). A second PR1 homologue from tomato, LsPR1–2, and two PR1 homologues from grape, VVPR1–1 and VVPR1–2, were isolated directly from the respective genomes by PCR based on the published genomic sequences. Other non-plant PR1 homologues were also obtained to assay for protection against FB1-induced PCD in transgenic tomato roots. The human glioma PR protein (GLIPR1) encoding sequence was purchased from the I.M.A.G.E. Consortium (Open Biosystems, Lafayette, CO, USA). The dog hookworm gene ancylostoma secreted protein (ASP) was provided by R. Hussey (University of Georgia, Athens, GA, USA). To check for RNA effects of the transcript, a mis-sense mutant version of P14 was made by PCR which shows deletion of base 49 of the coding sequence.

Transgenic tobacco plants

Nicotiana tabacum L. cv. Petit Havana SR1 transgenic plants were constructed to over-express the fusion of the 5' untranslated region (5' UTR) from P14a, the coding sequence of P14a and an additional 10 glycines between P14a and GFP, followed by the coding sequence of GFP and the 3' UTR from P14a driven by CaMV 35S. The 10 glycine spacer allows correct folding of the fusion protein.

California wild grape plants

California wild grape (*Vitis californica*) was grown under standard glasshouse conditions and inoculated with *Xf* as a control in Fig. 4. *Vitis californica* is recognized anecdotally as an asymptomatic *Vitis* host species, which was confirmed by our inoculation experiments, wherein the plants carried a low level of the bacteria and remained asymptomatic throughout the experiment.

Transgenic grape plants

Rhizobium tumefaciens strain LBA4404, containing the plant transforming binary plasmid for PR1 expression, was used by the University of California at Davis Parsons' Transformation Facility (<http://ucdptf.ucdavis.edu>) to transform and regenerate *Vitis vinifera* cv. Thompson seedless embryos according to the method of Agüero *et al.* (2015). Plants were verified for expression of the transgene by Northern analysis. Transgenic grape plants were transplanted to soil and grown in a glasshouse. After creating clones of transgenic lines for *Xf* inoculation studies, the plants were trained to grow with two canes prior to inoculation by periodic pruning of the side and top branches. Plants transformed with an EV were used as transgenic controls, as were wild-type untransformed Thompson Seedless plants.

RNA isolation and analysis

RNA was isolated from tobacco leaves with Trizol (Gibco, Grant Island, NY, USA) according to the manufacturer's specifications and from grape leaves using a cetyltrimethylammonium bromide (CTAB) extraction

Table 3 Primers used in this study.

Primer name	Sequence 5' to 3' (restriction site used for cloning underlined)	Comments
P14aF	GCGAATTCATGGGGTTGTTCAACATCTCATTGTTACTC	PCR F primer for P14a
P14aR	GCGCTCGAGAGTGAAGGACGTTGCCGATCCAGTTGCCTAC	PCR R primer for P14a
misS_P14	GCGAATTCATGGGGTTGTTCAACATCTCATTGTTACTCACTGTCTCATGGTA TTACCATATTTCACTCTTG	PCR F primer to delete base 49 of P14a
P14aNoLDF	GCGAATTCATGCAAAATTCACCCCAAGACTATCTTGGCGTTC	PCR F primer to remove secretory leader of P14a
SLPR1F	GCGAATTCACAACACTTAAATTTATTTCTCTCAAAGC	PCR F primer for SLPR1–2
SLPR1R	GCGCTCGAGAATAATTATTTGATCCCTTACACATC	PCR R primer for SLPR1–2
VVPR1-1F	GCGAATTCATGGGGTTGTGAGGAGTCCATTAGCACTCCTTTG	PCR F primer for VVPR1-1
VVPR1-1R	GCGCTCGAGTTAATAAGGACGTTGCCGATATAGTTGCC	PCR R primer for VVPR1-1
VVPR1–2F	GCGAATTCATGAGTCCATGGCACTGTGTTCTTGTCTACTAC	PCR F primer for VVPR1–2
VVPR1–2R	GCGCTCGAGTCAAGGCCTCTCCAATGTAATCCCAGGAG	PCR R primer for VVPR1–2
fusGFPfor	ACGTCCTTACGGAGGTGGAGGTGGAGGTGGAGGTGGAGGTATGTT GAGCAAGGGCGAGGA	PCR F GFP for P14a:GFP fusion adds gly10
fusP14rev	TGCTCACCATACCTCCACCTCCACCTCCACCTCCACCTCCGTAAGGACGTTG CCGATCC	PCR R P14a primer for P14a:GFP fusion
GFPF	GCGAATTCATGGTGGAGCAAGGGCGAGGAGCTGTT	PCR F GFP primer
GFP R	GCGCTCGAGTTACTTTGACAGCTCGTCCATGCCGT	PCR R GFP primer
P14a 3'UTR_F	GCGCTCGAGAATGATGTATACCTTATGACATGTTG	PCR F primer for P14a 3'UTR
P14a 3'UTR_R	GCGTCTAGACTAATTAATATATGCCATGC	PCR R primer for P14a 3'UTR
P14 5'UTR F RI	GCGAATTCACAATAACTTAGATTATTTCTCTGCACTAAACCTAAAGAAA AATGGGGTTGTTCAACATCTCA	PCR F primer for P14a 5'UTR
GLIPR1F	GCGAATTCATGCGTGTACACTTGTACAATAGCCTGGATGG	PCR F primer to move GLIPR1 to binary
GLIPR1R	GCGCTCGAGTTAGTCCAAAAGAACTAAATTAGGGTACTTGAGCTG	PCR R primer to move GLIPR1 to binary
qPCR Xf16S_F	AAAAATCGCCAACATAAACCCA	qPCR F primer for <i>Xf</i> detection
qPCR Xf 16S_R	CCAGGCGTCTCACAAAGTTAC	qPCR R primer for <i>Xf</i> detection

The listed primers were used in conventional polymerase chain reaction (PCR) for cloning and in quantitative PCR (qPCR) for *Xylella fastidiosa* (*Xf*) quantification. Underlined sequences denote added restriction sites. P14 and green fluorescent protein (GFP) were fused by overlap extension PCR.

protocol (landolino *et al.*, 2004). For Northern blots, 10 µg of total RNA was run on a formaldehyde gel and transferred to nylon membranes by capillary blot. RNA was detected using a Chemiluminescent Nucleic Acid Detection Kit (ThermoFisher Scientific #89880, Santa Clara, CA, USA). For PCR analysis, RNA was converted to cDNA by oligo dT priming and reverse transcriptase. PCRs were set up using the synthesized cDNA as template and specific pairs of primers designed against the putative transgene. The resulting products were separated by agarose gel electrophoresis.

Pseudomonas syringae pv. *tabaci*

Glasshouse-grown tobacco (*N. tabacum* cv. Xanthi) plants used for inoculations were 4–6 weeks old and had six to eight expanded leaves. *Pseudomonas syringae* pv. *tabaci*, grown overnight in Kings B medium, was adjusted to 10⁴ colony-forming units/mL. This diluted *Pseudomonas* was infiltrated into a tobacco leaf using a needle-less syringe. The leaf was infiltrated in an interveinal region by superficial wounding with a needle to improve infiltration, and then immediately placing a needle-less syringe over the puncture and holding a finger under the back of the leaf. Slow steady pressure was applied to infiltrate ~0.5 mL of culture.

Xylella fastidiosa (*Xf*)

The *Xf* strains used were Temecula and Stags Leap (gifts of Bruce Kirkpatrick and Andrew Walker (UC Davis, Davis, CA), respectively). After

7 days of growth on PD3 plates (Davis *et al.*, 1981), *Xf* colonies were scraped off and suspended in phosphate-buffered saline (PBS). *Xf* was diluted to OD₆₀₀ = 0.2–1.0 depending on the experiment, before placing a 20-µL drop of *Xf* suspension onto a grape cane, which was pierced with a 22G needle to allow the negative pressure of the xylem to pull the bacteria into the xylem.

Confocal microscopy

Tobacco leaf section images were obtained using two different confocal microscopes. A fresh unfixed section of leaf (2 cm × 2 cm) was cut from an intact leaf and immediately placed with water under a coverslip for imaging. Wild-type or mock-infiltrated leaves were used to set the baseline for all confocal microscopy. For Fig. 1, a confocal microscope (BioRad, Hercules, CA, USA, MRC1024) was used under 4× magnification by excitation at 488 nm with a krypton/argon 15-mW laser. The displayed colours in the computer-generated images represent the following: red denotes phenolic compounds in dying cells (Bennett *et al.*, 1996) (emission filter, 578–618 nm), green denotes GFP expression (emission filter, 506–538 nm) and blue denotes chlorophyll autofluorescence (emission filter, 664–696 nm). However, because of the breakdown of the BioRad microscope, a Leica TCS SPE confocal microscope was used for Fig. S1. These 20× Leica (Buffalo Grove, IL, USA) confocal images used a 488-nm diode laser and displayed chlorophyll as red using an emission filter of 675–725 nm, GFP as green using an emission filter of 475–525 nm and plant

cell death as blue using an emission filter of 625–650 nm. On the Leica microscope, overlap of emissions was represented by a third colour: red and blue as magenta, red and green as yellow, and blue and green as aqua.

Protein purification with His6 and P14a antibody production

The expression of 6 × His-tagged P14a protein in *Escherichia coli* was performed according to the manufacturer's instructions (Qiagen, Germantown, MD, USA). The elution fraction was resuspended in loading buffer and subjected to SDS-PAGE. The band at ~14 kDa was cut from the gel and sent to Spring Valley Laboratories, Inc., (Woodbine, MD, USA) for antibody production in rabbits. The specificity of the P14a antibody was shown by Western analysis of FB1-treated tomato tissues, which revealed a single ~14-kDa protein band at a dilution of 1 : 20 000 (data not shown). No comparable band was detected in the pre-bleed negative antibody control.

Affinity chromatography and mass spectrometry

Co-IPs were performed using the ProFound co-immunoprecipitation kit (Pierce #26149, Rockford, IL, USA). Anti-P14a antibody was coupled to Aminolink Plus gel according to the manufacturer's instructions. Immune complexes from both treatments were eluted from the resin, and 10- μ L samples were analysed by SDS-PAGE followed by immunoblot analysis (data not shown). A 10- μ L aliquot from both treatments was also analysed by SDS-PAGE and silver stained with the spectrometry-compatible Silver-SNAP kit (Pierce). No 15-kDa band indicative of P14a was retained and eluted from the no-antibody control column. Differentially expressed bands were then sent to the University of California at Davis proteomics facility for trypsin digest and LC-MS/MS analysis. All MS/MS samples were analysed using X! Tandem [version CYCLONE (2013.02.01.1)]. X! Tandem was set up to search the Solgenomics *Solanum lycopersicum* database (34 725 entries).

Criteria for protein identification

Scaffold (version 4.3.0, Proteome Software Inc., Portland, OR, USA) was used to validate MS/MS-based peptide and protein identifications.

Accession number

KT895376.1: synthetic mis-sense mutation in P14 coding sequence (CDS).
KT895375.1: synthetic P14-GFP fusion CDS.

ACKNOWLEDGEMENTS

We acknowledge the California Department of Food and Agriculture (CDFA-16-0559-SA).

REFERENCES

Murashige, T. and Skoog, F. (1962) A revised medium for rapid growth and bio assays with tobacco tissue cultures. *Physiol. Plant.* **15**, 473–497.
Agüero, C.B., Meredith, C.P. and Dandekar, A.M. (2015). Genetic transformation of *Vitis vinifera* L. cvs Thompson Seedless and Chardonnay with the pear PGIP and GFP encoding genes. *Vitis*, **45**, 1–8.

Antoniw, J.F. and White, R.F. (1986) Changes with time in the distribution of virus and PR protein around single local lesions of TMV infected tobacco. *Plant Mol. Biol.* **6**, 145–149.
Arca, B., Lombardo, F., Valenzuela, J.G., Francischetti, I.M.B., Marinotti, O., Coluzzi, M. and Ribeiro, J.M.C. (2005) An updated catalogue of salivary gland transcripts in the adult female mosquito, *Anopheles gambiae*. *J. Exp. Biol.* **208**, 3971–3986.
Asai, T., Stone, J.M., Heard, J.E., Kovtun, Y., Yorgey, P., Sheen, J. and Ausubel, F.M. (2000) Fumonisin B1-induced cell death in *Arabidopsis* protoplasts requires jasmonate-, ethylene-, and salicylate-dependent signaling pathways. *Plant Cell*, **12**, 1823–1835.
Ashida, H., Mimuro, H., Ogawa, M., Kobayashi, T., Sanada, T., Kim, M. and Sasakawa, C. (2011) Cell death and infection: a double-edged sword for host and pathogen survival. *J. Cell Biol.* **195**, 931–942.
Bennett, M., Gallagher, M., Fagg, J., Bestwick, C., Paul, T., Beale, M., and Mansfield, J. (1996) The hypersensitive reaction, membrane damage and accumulation of autofluorescent phenolics in lettuce cells challenged by *Bremia lactucae*. *Plant J.* **9**, 851–865.
Azevedo, C., Betsuyaku, S., Peart, J., Takahashi, A., Noël, L., Sadanandom, A., Casais, C., Parker, J. and Shirasu, K. (2006) Role of SGT1 in resistance protein accumulation in plant immunity. *EMBO J.* **25**, 2007–2016.
Chandran, D., Inada, N., Hather, G., Kleindt, C.K. and Wildermuth, M.C. (2010) Laser microdissection of *Arabidopsis* cells at the powdery mildew infection site reveals site-specific processes and regulators. *Proc. Natl. Acad. Sci. USA*, **107**, 460–465.
Clouse, S.D. and Gilchrist, D.G. (1987) Interaction of the ASC locus in F8 paired lines of tomato with *Alternaria alternata* f. sp. *lycopersici* and AAL-toxin. *Phytopathology*, **77**, 80–82.
Conrath, U. (2011) Molecular aspects of defence priming. *Trends Plant Sci.* **16**, 524–531.
Davis, M.J., Whitcomb, R.F. and A. G. Gillaspie, Jr. (1981). *Fastidious Bacteria of Plant Vascular Tissue and Invertebrates* (including so called rickettsia-like bacteria). Heidelberg: Springer-Verlag.
Davletova, S., Rizhsky, L., Liang, H.J., Zhong, S.Q., Oliver, D.J., Coutu, J., Shulaev, V., Schlauch, K. and Mittler, R. (2005) Cytosolic ascorbate peroxidase 1 is a central component of the reactive oxygen gene network of *Arabidopsis*. *Plant Cell*, **17**, 268–281.
Dickman, M.B. and de Figueiredo, P. (2013) Death be not proud—cell death control in plant fungal interactions. *PLoS Pathog.* **9**, e1003542.
Dickman, M., Williams, B., Li, Y., de Figueiredo, P. and Wolpert, T. (2017) Reassessing apoptosis in plants. *Nat. Plants*, **3**, 773–779.
Dixon, D., Cutt, J. and Klessig, D. (1991) Differential targeting of the tobacco PR-1 pathogenesis-related proteins to the extracellular space and vacuoles of crystal idioblasts. *EMBO J.* **10**, 1317–1324.
Dong, X. (2004) NPR1, all things considered. *Curr. Opin. Plant Biol.* **7**, 547–552.
Dongping, Z., Li, C., Bing, L.V. and Jiansheng, L. (2013) The scaffolding protein RACK1: a platform for diverse functions in the plant kingdom. *J. Plant Biol. Soil Health*, **1**, 7.
Elmore, S. (2007) Apoptosis: a review of programmed cell death. *Toxicol. Pathol.* **35**, 495–516.
Fu, Z.Q., Yan, S., Saleh, A., Wang, W., Ruble, J., Oka, N., Mohan, R., Spoel, S.H., Tada, Y., Zheng, N. and Dong, X. (2012) NPR3 and NPR4 are receptors for the immune signal salicylic acid in plants. *Nature*, **486**, 228–232.
Fuchs, Y. and Steller, H. (2011) Programmed cell death in animal development and disease. *Cell*, **147**, 742–758.
Fujiwara, M., Hamada, S., Hiratsuka, M., Fukao, Y., Kawasaki, T. and Shimamoto, K. (2009) Proteome analysis of detergent-resistant membranes (DRMs) associated with OsRac1-mediated innate immunity in rice. *Plant Cell Physiol.* **50**, 1191–1200.
Gibbs, G.M., Roelants, K. and O'Bryan, M.K. (2008) The CAP superfamily: cysteine-rich secretory proteins, antigen 5, and pathogenesis-related 1 proteins—roles in reproduction, cancer, and immune defense. *Endocr. Rev.* **29**, 865–897.
Gilchrist, D.G. (1997) Mycotoxins reveal connections between plants and animals in apoptosis and ceramide signaling. *Cell Death Differ.* **4**, 689–698.
Gilchrist, D.G. (1998) Programmed cell death in plant disease: the purpose and promise of cellular suicide. *Annu. Rev. Phytopathol.* **36**, 393–414.
Gilchrist, D.G., Lincoln, J.E. and Richael, C. (2001) *Inhibiting Apoptosis in Plants Using a Baculovirus p35 Protease Inhibitor Gene*. United States Patent Office Patent # 6310273, the University of California.

- Glazebrook, J. (2005). Contrasting mechanisms of defense against biotrophic and necrotrophic pathogens. *Annu. Rev. Phytopathol.* **43**, 205–227.
- Görlach, J., Volrath, S., Knauf-Beiter, G., Hengy, G., Beckhove, U., Kogel, K.H., Oostendorp, M., Staub, T., Ward, E., Kessmann, H. and Ryals, J. (1996). Benzothiadiazole, a novel class of inducers of systemic acquired resistance, activates gene expression and disease resistance in wheat. *Plant Cell*, **8**, 629–643.
- Gu, Y. and Innes, R.W. (2012) The KEEP ON GOING protein of *Arabidopsis* regulates intracellular protein trafficking and is degraded during fungal infection. *Plant Cell*, **24**, 4717.
- Harvey, J., Lincoln, J. and Gilchrist, D. (2008) Programmed cell death suppression in transformed plant tissue by tomato cDNAs identified from an *Agrobacterium rhizogenes*-based functional screen. *Mol. Genet. Genomics*, **279**, 509–521.
- Iakimova, E., Batchvarova, R., Kapchina-Toteva, V., Popov, T., Atanassov, A. and Woltering, E. (2004) Inhibition of apoptotic cell death induced by *Pseudomonas syringae* pv. *tabaci* and mycotoxin Fumonisin B1. *Biotechnol. Biotechnol. Equip.* **18**, 34–46.
- Iandolino, A.B., da Silva, F.G., Lim, H., Choi, H., Williams, L.E. and Cook, D.R. (2004) High-quality RNA, cDNA, and derived EST libraries from grapevine (*Vitis vinifera* L.). *Plant Mol. Biol. Rep.* **22**, 269–278.
- Islas-Flores, T., Rahman, A., Ullah, H. and Villanueva, M.A. (2015) The receptor for activated C kinase in plant signaling: tale of a promiscuous little molecule. *Front. Plant Sci.* **6**, 1090.
- Iwai, T., Seo, S., Mitsuhashi, I. and Ohashi, Y. (2007) Probenazole-induced accumulation of salicylic acid confers resistance to *Magnaporthe grisea* in adult rice plants. *Plant Cell Physiol.* **48**, 915–924.
- Jones, J.D.G. and Dangl, J.L. (2006) The plant immune system. *Nature*, **444**, 323–329.
- Kadota, Y. and Shirasu, K. (2012) The HSP90 complex of plants. *Biochim. Biophys. Acta*, **1823**, 689–697.
- Kinkema, M., Fan, W. and Dong, X. (2000) Nuclear localization of NPR1 is required for activation of PR gene expression. *Plant Cell*, **12**, 2339–2350.
- Lam, E. (2004) Controlled cell death, plant survival and development. *Nat. Rev. Mol. Cell Biol.* **5**, 305–315.
- Li, L., Yang, G., Ren, C., Tanimoto, R., Hirayama, T., Wang, J., Hawke, D., Kim, S.M., Lee, J.-S., Goltsov, A.A., Park, S., Ittmann, M.M., Troncoso, P. and Thompson, T.C. (2013) Glioma pathogenesis-related protein 1 induces prostate cancer cell death through Hsc70-mediated suppression of AURKA and TPX2. *Mol. Oncol.* **7**, 484–496.
- Lincoln, J.E., Richael, C., Overduin, B., Smith, K., Bostock, R. and Gilchrist, D.G. (2002) Expression of the antiapoptotic baculovirus p35 gene in tomato blocks programmed cell death and provides broad-spectrum resistance to disease. *Proc. Natl. Acad. Sci. USA*, **99**, 15 217–15 221.
- Lindsay, W.P., Lamb, C.J. and Dixon, R.A. (1993) Microbial recognition and activation of plant defense systems. *Trends Microbiol.* **1**, 181–187.
- Nakashima, A., Chen, L., Thao, N.P., Fujiwara, M., Wong, H.L., Kuwano, M., Umemura, K., Shirasu, K., Kawasaki, T. and Shimamoto, K. (2008). RACK1 functions in rice innate immunity by interacting with the rac1 immune complex. *Plant Cell*, **20**, 2265–2279.
- Niderman, T., Genetet, I., Bruyere, T., Gees, R., Stintzi, A., Legrand, M., Fritig, B. and Mosinger, E. (1995) Pathogenesis-related PR-1 proteins are antifungal. *Plant Physiol.* **108**, 17–27.
- Peart, J.R., Lu, R., Sadanandom, A., Malcuit, I., Moffett, P., Brice, D.C., Schauser, L., Jaggard, D.A.W., Xiao, S., Coleman, M.J., Dow, M., Jones, J.D.G., Shirasu, K. and Baulcombe, D.C. (2002) Ubiquitin ligase-associated protein SGT1 is required for host and nonhost disease resistance in plants. *Proc. Natl. Acad. Sci. USA*, **99**, 10 865–10 869.
- Pečenková, T., Pleskot, R. and Žárský, V. (2017) Subcellular localization of *Arabidopsis* pathogenesis-related 1 (PR1) protein. *Int. J. Mol. Sci.* **18**, 825.
- Reape, T.J., Molony, E.M. and McCabe, P.F. (2008) Programmed cell death in plants: distinguishing between different modes. *J. Exp. Bot.* **59**, 435–444.
- Ribeiro, R. de L.D., Hagedorn, D.J., Durbin, R.D. and Uchytíl, T.F. (1979) Characterization of the bacterium inciting bean wildfire in Brazil. *Phytopathology*, **69**, 208–212.
- Richael, C. and Gilchrist, D. (1999) The hypersensitive response: a case of hold or fold? *Physiol. Mol. Plant Pathol.* **55**, 5–12.
- Richael, C., Lincoln, J.E., Bostock, R.M. and Gilchrist, D.G. (2001) Caspase inhibitors reduce symptom development and limit bacterial proliferation in susceptible plant tissues. *Physiol. Mol. Plant Pathol.* **59**, 213–221.
- Saraste, A. and Pulkki, K. (2000) Morphologic and biochemical hallmarks of apoptosis. *Cardiovasc. Res.* **45**, 528–537.
- Sarowar, S., Kim, Y.J., Kim, E.N., Kim, K.D., Hwang, B.K., Islam, R. and Shin, J.S. (2005) Overexpression of a pepper basic pathogenesis-related protein 1 gene in tobacco plants enhances resistance to heavy metal and pathogen stresses. *Plant Cell Rep.* **24**, 216–224.
- Schuren, F.H.J., Asgeirsdottir, S.A., Kothe, E.M., Scheer, J.M.J. and Wessels, J.G.H. (1993) The Sc7/Sc14 gene family of *Schizophyllum commune* codes for extracellular proteins specifically expressed during fruit-body formation. *J. Gen. Microbiol.* **139**, 2083–2090.
- Schwab, R., Palatnik, J.F., Riester, M., Schommer, C., Schmid, M. and Weigel, D. (2005). Specific effects of microRNAs on the plant transcriptome. *Dev. Cell*, **8**, 517–527.
- Serino, G. and Deng, X.-W. (2007) Protein coimmunoprecipitation in *Arabidopsis*. *Cold Spring Harb. Protoc.* **2007**, pdb.prot4683.
- Shirasu, K. (2009) The HSP90-SGT1 chaperone complex for NLR immune sensors. *Annu. Rev. Plant Biol.* **60**, 139–164.
- Stone, J.M., Heard, J.E., Asai, T. and Ausubel, F.M. (2000) Simulation of fungal-mediated cell death by Fumonisin B1 and selection of Fumonisin B1-resistant (*fb*) *Arabidopsis* mutants. *Plant Cell*, **12**, 1811–1822.
- Teixeira, P.J.P.L., Thomazella, D.P.T., Vidal, R.O., do Prado, P.F.V., Reis, O., Baroni, R.M., Franco, S.F., Mieczkowski, P., Pereira, G.A.G. and Mondego, J.M.C. (2012) The fungal pathogen *Moniliophthora perniciosa* has genes similar to plant PR-1 that are highly expressed during its interaction with Cacao. *PLoS One*, **7**, e45929.
- van Doorn, W.G. and Woltering, E.J. (2005) Many ways to exit? Cell death categories in plants. *Trends Plant Sci.* **10**, 117–122.
- van Loon, L.C. (1997) Induced resistance in plants and the role of pathogenesis-related proteins. *Eur. J. Plant Pathol.* **103**, 753–765.
- van Loon, L.C., Rep, M. and Pieterse, C.M.J. (2006) Significance of inducible defense-related proteins in infected plants. *Annu. Rev. Phytopathol.* **44**, 135–162.
- van Loon, L. and van Kammen, A. (1970) Polyacrylamide disc electrophoresis of the soluble leaf proteins from *Nicotiana tabacum* var. 'Sansum' and 'Sansum NN#'. II. Changes in protein constitution after infection with tobacco mosaic virus. *Virology*, **40**, 199–211.
- van Loon, L.C. and van Strien, E.A. (1999) The families of pathogenesis-related proteins, their activities, and comparative analysis of PR-1 type proteins. *Physiol. Mol. Plant Pathol.* **55**, 85–97.
- Wang, H., Li, J., Bostock, R.M. and Gilchrist, D.G. (1996) Apoptosis: a functional paradigm for programmed plant cell death induced by a host-selective phytotoxin and invoked during development. *Plant Cell*, **8**, 375–391.
- Wang, K., Uppalapati, S.R., Zhu, X., Dinesh-Kumar, S.P. and Mysore, K.S. (2010) SGT1 positively regulates the process of plant cell death during both compatible and incompatible plant–pathogen interactions. *Mol. Plant Pathol.* **11**, 597–611.
- Watanabe, S., Shimada, T.L., Hiruma, K. and Takano, Y. (2013) Pathogen infection trial increases the secretion of proteins localized in the endoplasmic reticulum body of *Arabidopsis*. *Plant Physiol.* **163**, 659.

SUPPORTING INFORMATION

Additional Supporting Information may be found in the online version of this article at the publisher's website:

Fig. S1 *Pseudomonas syringae* pv. *tabaci* localization. P14a-GFP transgenic tobacco (*Nicotiana tabacum*) leaves into which *P. syringae* pv. *tabaci* was infiltrated differ in that (A) was infiltrated with wild-type bacteria, whereas (B) was infiltrated with green fluorescent protein (GFP)-tagged bacteria. The respective tissues were imaged with a confocal microscope after 7 days. These images were recorded with a Leica confocal microscope at 20× magnification by a 488-nm diode laser that displayed chlorophyll as red using an emission filter of 675–725 nm. GFP appears as green using an emission filter of 475–525 nm and plant cell death appears as blue using an emission filter of 625–650 nm. The overlap of each pair of emissions is represented by Leica as a third colour, i.e. red and blue as magenta,

red and green as yellow, and blue and green as aqua. The difference is that the image in (A) reveals expressed GFP from transgenic plant cells only, whereas the image in (B) shows both GFP-tagged *Pseudomonas* and GFP-tagged P14A fusion protein as aqua (green on top of blue).

Table S1 Lanes 1–7 correspond to the seven bands extracted from the samples treated with Fumonisin B1 (FB1) (see Fig. 5,

lane 2). Lane 1 corresponds to the smallest band (~15 kDa), whereas lane 7 corresponds to the largest band (~100 kDa). Lanes 8–14 correspond to the seven bands extracted from the control samples (no FB1; Fig. 5, lane 1), which represent the same regions as the samples treated with FB1. The number of identified peptides appears in each box under a given lane.